Velocities of deepwater reservoir sands

De-Hua Han, University of Houston, USA
M. Batzle, Colorado School of Mines, Golden, USA

Deepwater reservoirs, those in water depths ranging from 1000 m to more than 3000 m, often consist of young turbidite sediments associated with early hydrocarbon charge, overpressure buildup, and seal with retarded diagenesis. Deepwater sands maintain shallow properties even at great depths (e.g., 18 000 ft) but these weakly cemented sands—with a history of progressive compaction and cementation—differ from surface sediments.

Current understanding of the properties of deepwater sands, mainly based on log and seismic data, has proved insufficient and risky. In 1998, the GDC team showed a statistical distribution of velocity and density of deepwater sands as a function of depth relative to seafloor depth. These data revealed a general compaction (depth) effect on sand properties. However, significant scattering in the data suggests many parameters need to be further examined.

Spencer and Thompson (1994) showed that the acoustic properties of loose sands are controlled by grain contacts. Han (1994) demonstrated that the shear-wave velocities are particularly sensitive to weak cementation. Han (1986), Marion et al. (1992), and Yin (1992) have systematically investigated porosity/velocity of various mixtures of loose sands and clays. The results have revealed a gradual effect of clay content on porosity and velocity which has been used to simulate properties of shaly sands and sandy shales. Zimmer et al. (2002) studied velocities of packed sands and glass beads with different sorting combinations. The data showed a significant effect of pressure on velocities and a sorting effect on porosity.

However, sediment compaction is not an elastic process. Both pressure and time of duration on sediments affect compaction. Laboratory compaction, done in days, may not simulate natural compaction which occurs over millions of years. Thus, the general applicability to deepwater sands of results based on such data is questionable.

In contrast, the results in this study are based on measurements of a suite of sand samples from the Gulf of Mexico. Although the samples are limited, we feel the results are significant and might suggest a DHI.

Texture of deepwater sands. The core samples come from two wells in water depths of 4000 ft and two reservoir formations at depths of 12 000 ft (shallow) and 17 700 ft (deep). Both reservoir sands were overpressured with differential pressure (overburden pressure minus pore pressure) around 2000 psi (13.8 MPa) for the shallow sands and 4000 psi (27.6 MPa) for the deep sands.

Figure 1 shows that the porosity, bulk, and grain density of samples are differentiated into three distinct groups by porosity. These include a group of eight shallow samples with very high porosity (VHP) of 30-35% and a group of 17 deep samples with high porosity (HP) of 24-30%. The third group, low-porosity samples (< 20%), are silt and shale, which is not the focus for this study.

Deep samples with low porosity might have been subjected to more compaction and cementation than shallow samples. For the samples from the same formation, the range of porosity is related to sample sorting—high-porosity samples may have had better initial sorting than low-porosity samples from similar depth.

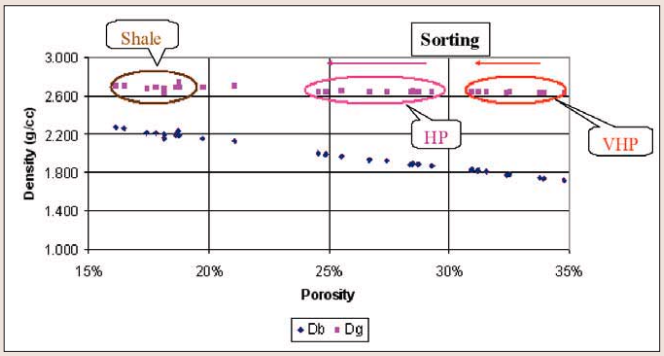

Figure 1. Dry-bulk and grain density as a function of porosity for the shallow (12 000-ft) and deep (17 700-ft) sands.

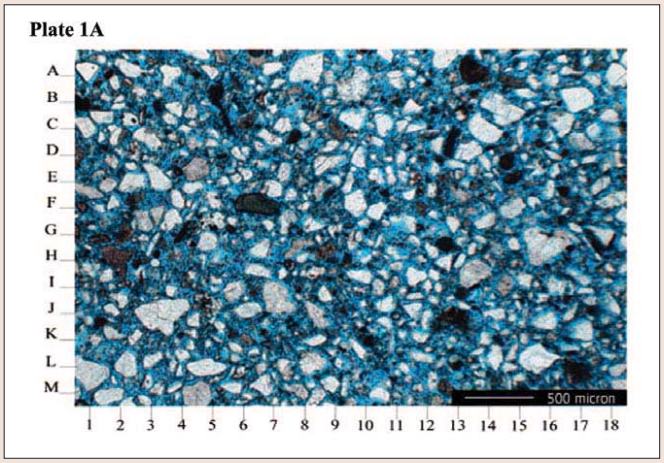

Figure 2. Thin section for a deepwater clean, unconsolidated fine sand sample.

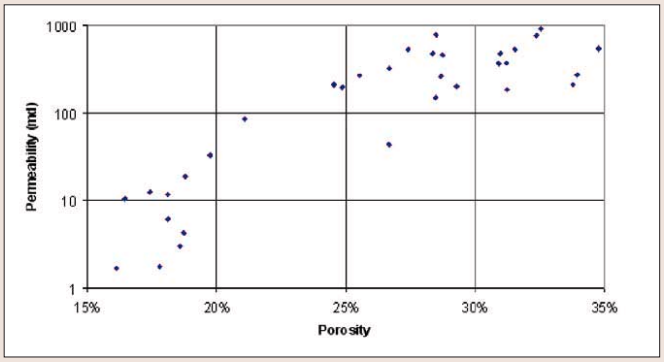

Figure 3. Permeability versus porosity for the shallow and deep sands and shales.

All samples are relatively clean, fine-grained sands with no cementation (Figure 2). Grain density is about 2.65 g/cc, typical for clean sands. Dry bulk density decreases linearly with porosity. Measured gas permeability typically ranged from 100 to 1000 md (Figure 3).

Although the samples are unconsolidated, the measured data suggest that they have maintained in-situ grain packing and structures with negligible damage during coring and pressure release processes. Porosity measured at room pressure is higher than that at in-situ differential pressure con-

ditions. Our data show that after conditioning prepressure to that in situ, the effect of pressure cycling is limited, especially on velocities. We also measured total porosity reduction with in-situ differential pressure (Figure 4). In this case, porosity reduction ranged from 1 to 2% porosity unit for the in-situ differential pressure (2000 psi and 4000 psi for the shallow and the deep sands, respectively). The porosity reduction shows no relation to the porosity and is less dependent on the in-situ differential pressure. This may reveal that porosity relaxation due to the in-situ pressure relaxation is a unique measure of the degree of compaction and cementation of the rock frame. The measured porosity reduction in deepwater sands with in-situ packing and structure is significantly less than 3-4% porosity unit, which has been observed on laboratory-packed samples. These data reveal that the porosity reduction may be an indicator for the integrity and damage of core samples. The total porosity reduction (3–4%) measured on shaly and shale samples is much higher than on sand samples although porosity of shale samples at room pressure is significantly lower.

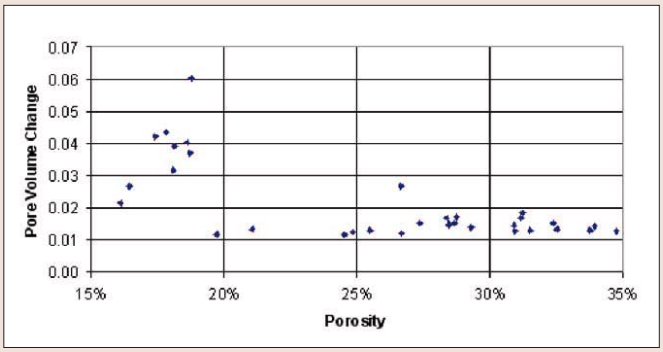

Figure 4. Total pore volume reduction is around 1.5% porosity unit for deepwater sands with no relation to porosity. There is much higher porosity reduction for shaly sands and shales.

Velocity measurements. Figure 5 shows that, for dry and brine-saturated sands, both V_P and V_S tend to increase with increasing pressure. The velocity increment is high at low pressure and low at high pressure. The effect of pressure on velocities can be modeled by a power law

$$V_P = a * P^{1/b} \quad (1)$$

where a is velocity at unit pressure. In the grain contact model (Mindlin, 1949), b equals 6. For loose-sand samples, grain contact is not perfect and tends to be better with increasing pressure compaction. We have observed that the b value of deepwater sand samples is in general around 6 or less, and can be as small as 4.5. The lower b value is similar to that of laboratory-packed sand samples. The higher b value suggests better grain contact and less pressure dependence on velocity. Dry S-wave velocity shows a slightly greater b value. Brine saturation stiffens the sand frame and increases bulk density, which causes an increase of P-wave velocity and a decrease of S-wave velocity. It also causes less pressure dependence on velocity. The b value for brine-saturated P-wave velocity increases to more than 15, which suggests significant reduction of the pressure dependence of P-wave velocity. However, the pressure dependence of S-wave velocity is only slightly affected.

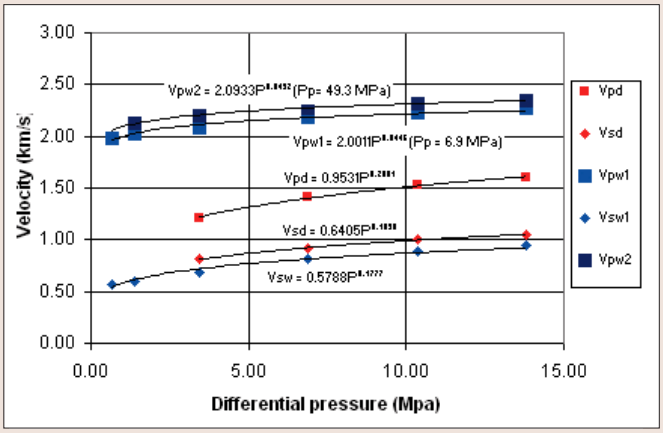

Figure 5. Measured dry and brine-saturated P- and S-wave velocities on a typical deepwater sand sample (for about 12 000 ft) as a function of differential pressure.

Figure 6 shows dry P- and S-wave velocity as a function of porosity. These data also include repackaged loose sands (LS) samples from damaged (collapsed) core samples, and data lines covered porosity from 24 to 40% and differential pressures of 0.05, 3.45, and 20 MPa for loose sand and glass bead samples (LGS) (Zimmer et al., 2002). P- and S-wave velocities of shallow sands are significantly lower than those of deep sands, although the upper limit of pressure is 13.8 MPa for the shallow sands and 27.6 MPa for the deep sands. Both the V_P and V_S of the VHP sands data show remarkable consistency with data of the LS sands and the LGS lines. But porosity compaction of the naturally compacted VHP sands is much smaller than repackaged samples. The VHP samples also show that velocities at differential pressure of 13.8 MPa are consistent with the velocity trend of the LGS samples at differential pressure of 20 MPa. And the velocities of the VHP samples at differential pressure of 3.45 MPa are higher than that of LS and LGS sands. These results suggest that the VHP sands are in an early compaction stage, and the velocities show a transition behavior from the repacked loose sands (the LS and the LGS sands). However, the HP sands—with more

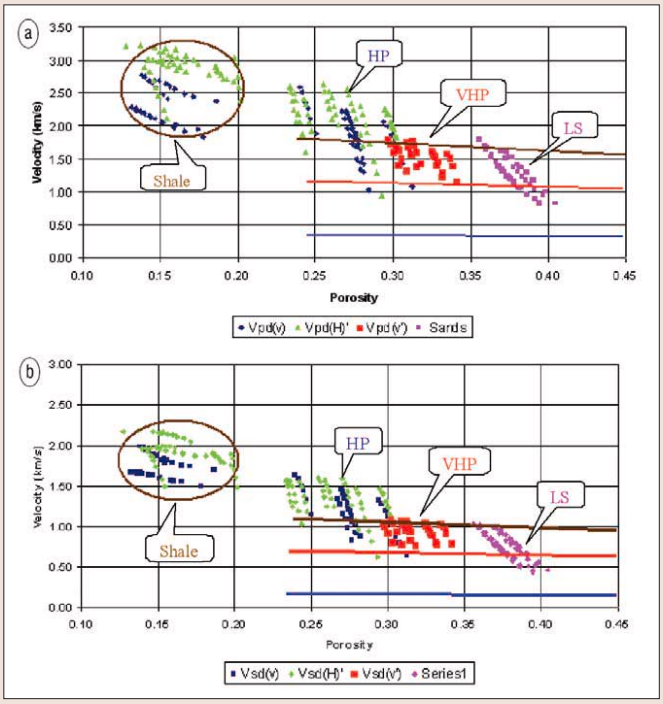

Figure 6. (a) Measured dry V_P versus porosity. (b) Measured dry V_S versus porosity.

compaction (low porosity) at deeper depths—show a significantly high-velocity trend (take off the pressure effect). S-wave velocities of the VHP sands show less relevance to porosity and are around 1.0 km/s, significantly less than for the deep

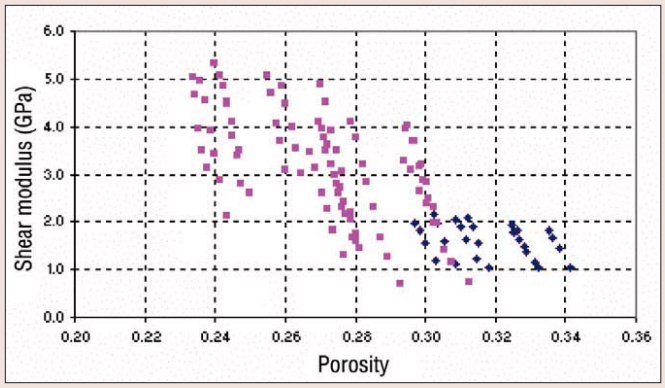

Figure 7. The HP (deep) sands have much higher shear modulus than those of the VHP (shallow) sands.

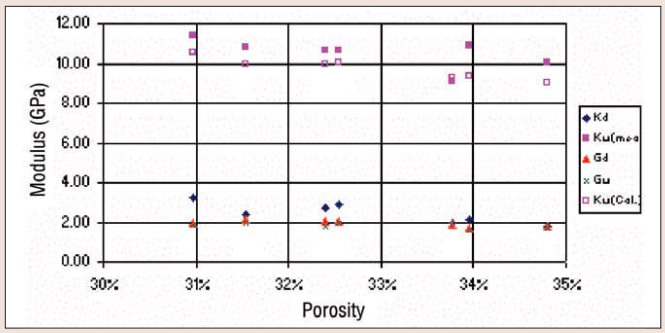

Figure 8. Measured dry and brine-saturated bulk and shear modulus of the VHP sand samples in comparison to modulus calculated with Gassmann's equation.

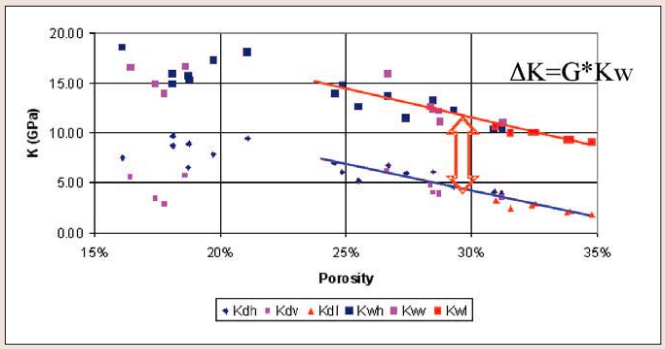

Figure 9. Dry and water-saturated bulk modulus.

sands. Significant separation in shear velocity of the VHP (shallow) from HP (deep) sands suggests that effects of compaction and cementation are mainly to stiffen sand rigidity for deep sands (Figure 7).

We concluded from these data that velocities of the VHP sands are less pressure-dependent than the HP (deep) sands. That may not represent in-situ conditions and might possibly be induced by core damage on the HP sands during coring. With high pressure in situ, the rock frame is stronger due to additional cementation. When pressure is released during coring, weak cement can be cracked due to extensional residual stress caused by relaxation of grain deformation. These induced cracks can cause the high-pressure effect on velocities, but this is not the case for loose sand samples.

Effect of fluid saturation on velocities. We measured velocities on brine-saturated samples to examine the effect of fluid saturation.

We first examined the fluid-saturation effect on the shear modulus. Figure 8 shows measured and calculated modulus of VHP sand samples at a differential pressure of 2000 psi. These data suggest that shear modulus remains constant, as predicted by Gassmann's equation, with water saturation for the sand samples. The data also show that the shear modulus is equal to or slightly less than the dry bulk modulus.

We compared the brine-saturated bulk modulus based on measured dry velocities calculated with Gassmann's equation to the bulk modulus based on measured brine-saturated velocities. The calculated modulus is a few percentage points lower. Data measured on the deep (HP) sands showed a similar trend. We conclude that velocity dispersion is minimal for those porous sands.

The fluid-saturation effect is mainly on the bulk modulus as shown in the simplified Gassmann's equation (Han and Batzle, 2004):

$$K_s = K_d + G(\phi) * K_f \tag{2}$$

Here $G(\phi)$ is the gain function, which is a dry rock frame property. Figure 9 shows dry and brine-saturated bulk modulus at high pressure.

Data show that dry bulk modulus increases significantly with decreasing porosity: 2.0 GPa at porosity of 35% to 7.0 GPa at porosity of 24%. The brine saturation causes a significant increase of bulk modulus. However, the increment of ΔK tends to be a constant and not sensitive to porosity. Consequently, we can use the increment in bulk modulus ΔK_d to calculate the gain function.

$$G(\phi) = \Delta K_d / K_f \tag{3}$$

Figure 10 shows the gain function for the shallow (VHP) and deep (HP) sand. The gain function for deepwater unconsolidated sands is distributed in a narrow range with the upper bound derived from the Reuss bound and the lower bound constant around 2.5. The gain function decreases with increasing pressure and seems more sensitive to pressure for the HP sands (core damage effect?) than the VHP sands. The lower bound of the gain function seems consistent with

$$G = D^2 * \phi * (2 - D * \phi)^2; \quad D = 2.1 \tag{4}$$

The gain function for the loose sands is significantly higher than those of consolidated reservoir sandstones (Han and Batzle, 2003).

Figure 11 shows that brine-saturated velocity is less dependent on porosity. We have developed an empirical model based on Reuss bound to model velocities. The Reuss bound of P-wave modulus is

$$M_{\text{Reuss}} = \frac{M_0}{1 + \left(M_0 / K_f - 1 \right) * \varphi} \tag{5}$$

We can derive P-wave velocity as

$$V_P = (M / \rho)^{0.5} = \left(\left(\frac{M_0}{1 + n * \varphi} \right) / \rho \right)^{0.5} \tag{6}$$

where M_0 is P-wave mineral modulus, and assumed equal to 83 GPa. The coefficient n is used to simulate different pressure effect on velocities. For S-wave velocity, a similar model can be used by replacing M_0 with grain shear modulus μ_0 (assume μ_0 is equal to 33 Gpa). This formulation is purely empirical and may be used to describe velocity-pressure-

porosity relations. The n value can be calibrated locally.

Zimmer et al. (2002) used the modified Reuss model (Dvorkin and Nur, 1996) to simulate the sorting effect on dry velocity-porosity relation for packaged sand samples. We found that their method is not proper for our data because geologic compaction affects the dry velocity-porosity relation of deepwater sands. The laboratory-packed (LS and LGS) sand samples show a sorting effect to reduce porosity, and almost no effect on dry velocities, but a large brine-saturation effect on P-wave velocity of poorly sorted, low-porosity sands. In comparison with laboratory-packed samples, deepwater sands show limited sorting effect and more geologic compaction effect: Dry velocities of deepwater sands are significantly higher than those of the LS and LGS sands, and increase with decreasing porosity. The brine-saturation effect on bulk modulus remains a constant (constant gain function). Consequently, water-saturated velocities more or less follow the Reuss trend and are less dependent on porosity.

P-wave and S-wave relationship. Dry P- and S-wave (shear) modulus are related to V_P/V_S ratio as follows:

$$\frac{M}{\mu} = \frac{V_P^2}{V_S^2} \tag{7}$$

Figure 12 plots dry shear and P-wave modulus with regression relationship as

$$\mu = -0.0035 * M^2 + 0.4399 * M - 0.1583 \tag{8}$$

The relation can be used to derive dry shear modulus from the dry P-wave modulus. At high pressure, the shear modulus tends to be linearly proportional to P-wave modulus (the red line in Figure 12) with a ratio of 0.42. This ratio is equivalent to the k/μ ratio of 1.05. This value tends to increase with decreasing differential pressure. This tight relationship between dry bulk and shear modulus provides an internal constraint on fluid-saturation effects on velocity.

Figure 13 shows measured V_P/V_S ratio versus porosity for dry and brine-saturated samples. The data reveal that dry V_P/V_S ratio is around 1.6 and did not show significant relation with porosity except that it slightly increased with decreasing porosity for samples from the same formation. Under brine-saturated conditions, V_P/V_S ratio (~2.1) for the deep HP sands is significantly less than for (~2.5) shallow VHP sands. This is due to less compaction and no cementation for the shallow VHP sands with low shear modulus and high porosity. The data also show that the HP water-saturated sands have V_P/V_S ratio that is similar to nearby shale samples.

Hydrocarbon indicators in deepwater sands. Many hydrocarbon indicators have been proposed (Russell et al., 2003). We propose a DHI with clear physical meaning. In order to identify the fluid from seismic, the key is the sensitivity of fluid effect on P-wave modulus given as:

$$M_s = M_d + G * K_f \tag{9}$$

For deepwater, turbidite, unconsolidated sand reservoirs, we can apply the above results to obtain a new hydrocarbon indicator. Assuming, we can determine the porosity of sand frame, bulk modulus of pore fluid (brine) and grain (mineral) modulus, from P-wave modulus of brine-saturated sands, we can calculate dry rock frame properties based on Gassmann's

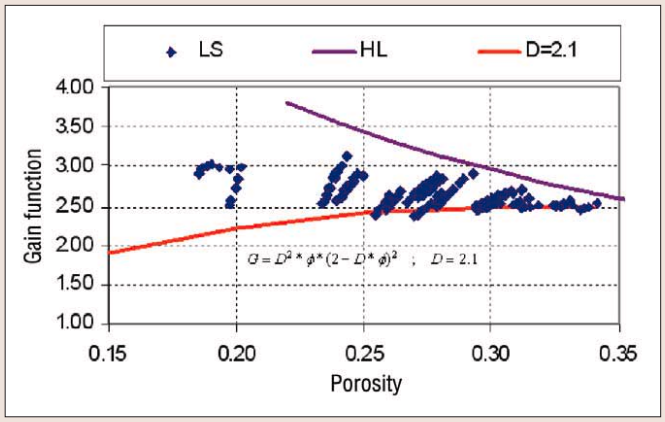

Figure 10. *Derived gain function versus porosity. Low bound of the gain function for deepwater sands is around 2.5.*

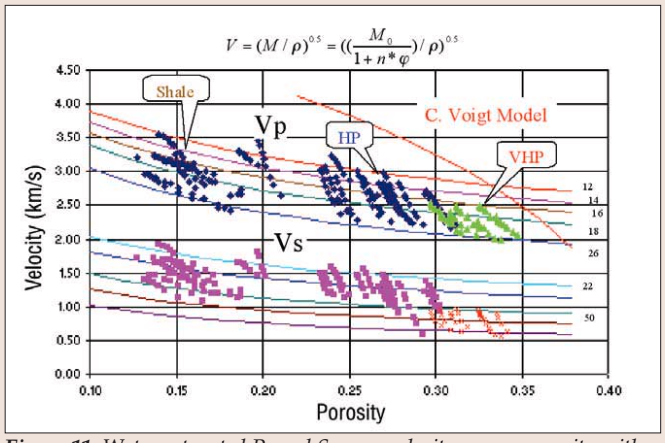

Figure 11. *Water saturated P- and S-wave velocity versus porosity with modeled velocity/porosity trend.*

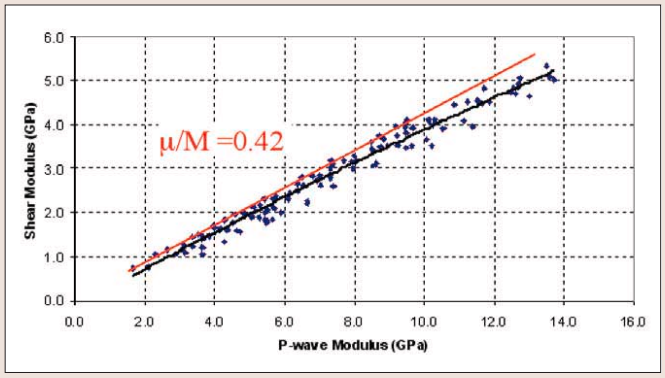

Figure 12. *Shear and P-velocity modulus relation.*

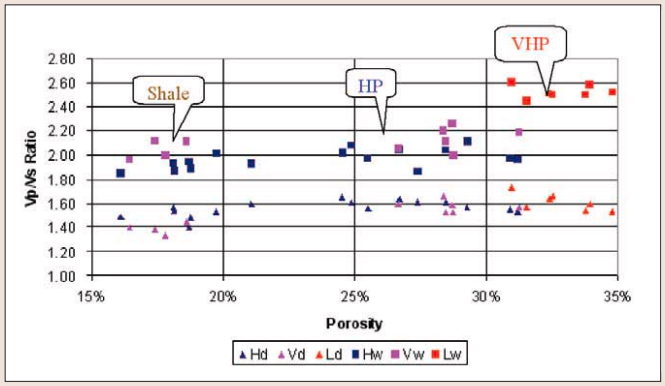

Figure 13. *Measured dry and brine-saturated V_P/V_S ratio for the shallow (VHP) and deep (HP) sands.*

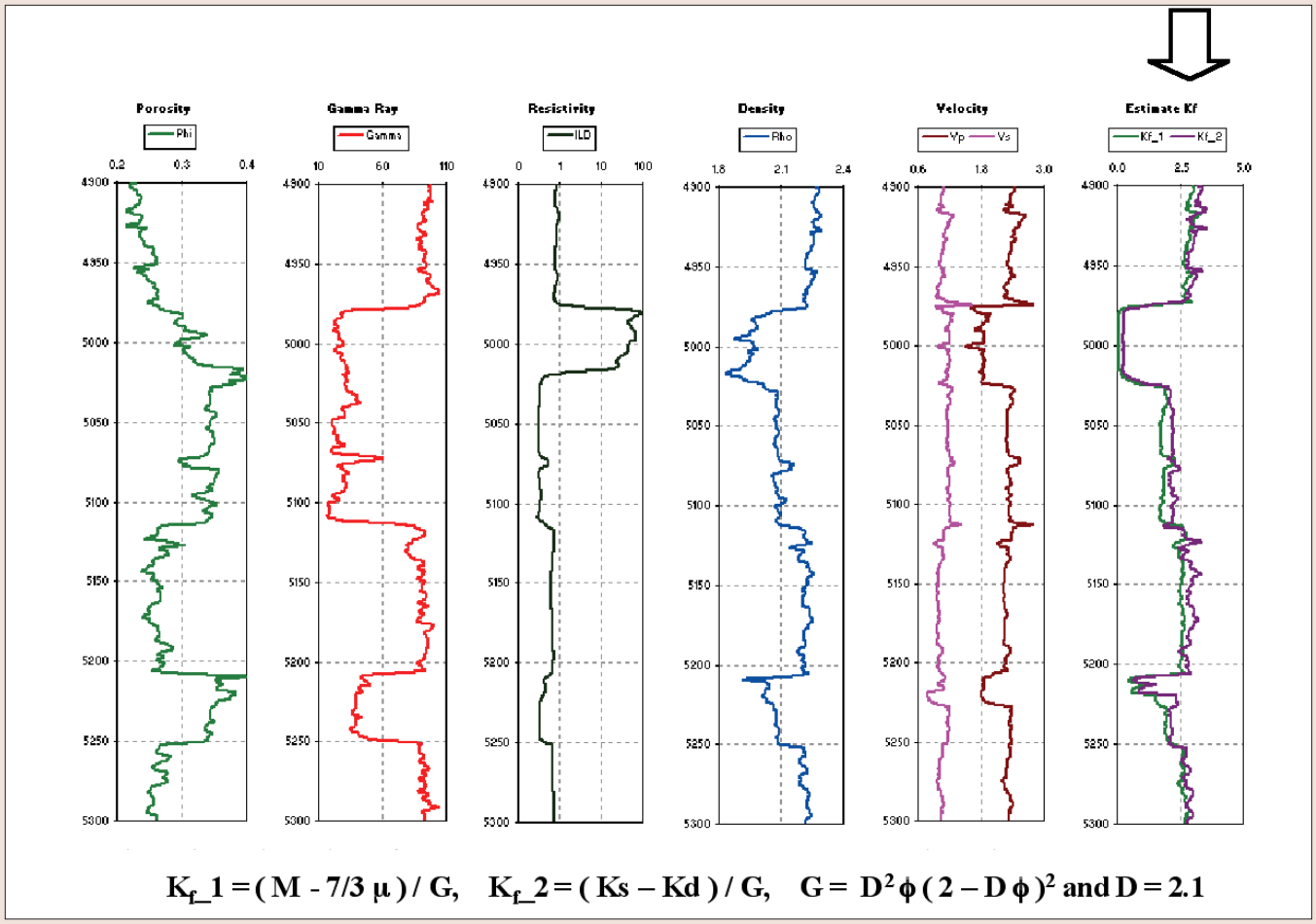

Figure 14. *Pore fluid bulk modulus for wet and gas formation derived from log data.*

equation—actually the modified Gassmann's equation with P-wave modulus (Han and Batzle, 2004). The brine-saturation effect (ΔK, or fluid factor) should be consistent with brine modulus and the gain function. The dry rock frame properties should be consistent with the measured data trend. By applying the gain function, we can directly calculate brine modulus, which should be consistent with the true in-situ value. With properties of dry rock frame we could also estimate hydrocarbon-saturation effect, or estimate fluid modulus based on P-wave modulus of reservoir sands and the gain function. Figure 14 shows estimated fluid modulus for a log data. Results show that we can directly estimate realistic brine modulus from wet zones and pore fluid modulus from gas zones. In the shale zone, brine modulus is overestimated due to applying the gain function for sands. An abnormally high brine modulus is a good lithology (shale) indicator.

We also compared different hydrocarbon indicators for deepwater environment (Figure 15). We have calculated 15 hydrocarbon attributes for gas (90% gas, 10% brine), fizz gas (90% brine, 10% gas), and brine sands. In comparison with brine-saturated sands (background), five attributes (ΔK, $\lambda^*\rho$, $\rho^*\Delta K$, ρ^*K_f and K_f) show higher but similar sensitivity to differentiate gas from fizz gas and wet sands. And the sensitivity of all attributes is basically determined by the fluid modulus (K_f). Clearly, in order to obtain accurate, meaningful interpretation of seismic attributes or forward modeling, we have to better understand measurements and models for hydrocarbon fluid properties. We have not yet been able to extract fluid modulus from seismic data. However, with improved seismic data and constraints from rock and fluid parameters, we expect to map pore fluid modulus based on seismic data in the near future.

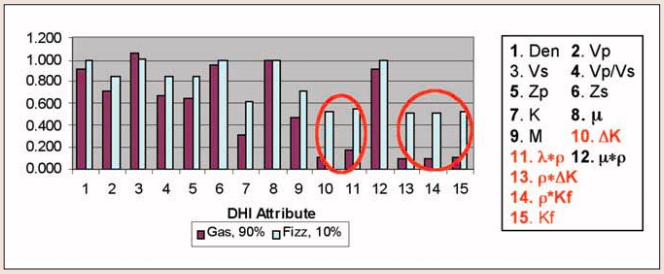

Figure 15. *For deepwater sands, relative sensitivity of 15 seismic attributes from a fizz gas (10% gas) and gas (90%) sands normalized with those of wet sands.*

Here, we discuss only elastic seismic attributes related to hydrocarbon fluids. Seismic wave dispersion and attenuation are also associated with hydrocarbon fluid saturation but via a very different mechanism. Greater wave dispersion and attenuation are especially associated with fizz gas saturation, which can used as additional hydrocarbon indicators. We will discuss them in a future paper.

Conclusion. Deepwater reservoir sands with unique sedimentary processes show progressive effect of compaction and cementation on porosity and frame velocities, which also incorporates the grain texture and fluid migration.

1) Compaction is a major driving force. Poor sorting will provide room for low initial packing porosity and more potential for continued compaction.
2) For deepwater sands, overpressure and early charge of hydrocarbon often block pore fluid flow and minimize the

cementation effect.

3) With increasing depth and age, porosity reduces and dry velocities increase. The effect of fluid saturation on the modulus of deepwater sands can be estimated by a constant fluid factor: the constant gain function (2.5) times the fluid modulus.
4) Velocity dispersion in deepwater sands is relatively small.
5) Compaction and weak cementation increase shear rigidity more than bulk modulus.
6) P- and S-wave velocities of water-saturated sands follow the Reuss trend, and show less dependence on porosity.
7) The effect of pressure on the velocity of VHP sands is relatively small. With weak cementation, the effect of pressure on velocity increases, which may be caused by core damage.
8) The dry shear modulus at high pressure is proportional to P-wave modulus.

The sensitivity of elastic seismic attributes to hydrocarbon saturation is basically controlled by the pore fluid modulus. The greater the difference of pore fluid modulus leads to a greater differential in seismic attributes, and greater potential to differentiate pore fluids seismically. However, it is also constrained by the degree of compaction and cementation of sand frame. More compaction and cementation equals less potential to differentiate different pore fluids. Therefore, we can conclude that detecting a shallow gas reservoir is relatively easier, but differentiating a gas from fizz reservoir is harder. For deepwater loose sand reservoirs with high pore pressure, we may be able to detect a gas reservoir and differentiate gas from fizz gas reservoirs. Potentially, we can map pore fluid modulus directly from seismic data. However, with increasing depth and age, as well as compaction and cementation, the elastic seismic attributes of sand formation tend to be less sensitive to saturations of different fluids. We will have less ability to detect gas reservoirs and more difficulty in differentiating gas and fizz gas reservoirs.

Suggested reading. "Elasticity of high-porosity sandstones: Theory for two North Sea data sets" by Dvorkin and Nur (GEOPHYSICS, 1996). "Rock property framework for comprehending deep-water seismic response" by GDC team (GSH 1998 Spring Symposium). *Effects of Porosity and Clay Content on Acoustic Properties of Sandstones and Unconsolidated Sediments* by Han (PhD dissertation, Stanford University, 1986). "Weak cementation effect on velocity of sands" by Han (SEG 1994 *Expanded Abstracts*). "Gain function and hydrocarbon indicators" by Han and Batzle (SEG 2003 *Expanded Abstracts*). "Gassmann's equation and fluid saturation effects on seismic velocities" by Han and Batzle (GEOPHYSICS, 2004). "Compliance of elastic bodies in contact" by Mindlin (*Journal of Applied Mechanics*, 1949). "Compressional velocity and porosity in sand clay mixtures" by Marion et al. (GEOPHYSICS, 1992). "Fluid-property discrimination with AVO: A Biot-Gassmann perspective" by Russell et al. (GEOPHYSICS, 2003). "Frame moduli of unconsolidated sands and sandstones" by Spencer and Thompson (GEOPHYSICS, 1994). *Acoustic Velocity and Attenuation of Rocks: Isotropy, Intrinsic Anisotropy, and Stress-Induced Anisotropy* by Yin (PhD dissertation, Stanford University, 1992). "Empirical pressure trends in unconsolidated sands" by Zimmer et al. (SEG 2002 *Expanded Abstracts*). TLE

Acknowledgments: We are grateful to Kerr-McGee for providing the core samples for this study and for the support of the Department of Energy (award DE-FC26-02NT15342) and of the corporate-sponsored Fluids/DHI Consortium.

Corresponding author: De-Hua.Han@mail.uh.edu